New Family of Three-Dimensional Topological Insulators with Antiperovskite Structure

Yan Sun,[1] Xing-Qiu Chen,[1,*] Seiji Yunoki,[2] Dianzhong Li,[1] and Yiyi Li[1]

[1]*Shenyang National Laboratory for Materials Science, Institute of Metal Research, Chinese Academy of Sciences, Shenyang 110016, China*

[2]*Computational Condensed Matter Physics Laboratory, RIKEN ASI, Saitama 351-0198, Japan, and CREST, Japan Science and Technology Agency (JST), Saitama 332-0012, Japan*

(Received 11 August 2010; revised manuscript received 13 October 2010; published 17 November 2010)

All known topological insulators are crystallographically related to either the noncentrosymmetric zinc-blende HgTe-type family or to the hexagonal centrosymmetric Bi_2Se_3 one. Through first-principles calculations, here we show evidence that under a proper uniaxial strain cubic ternary centrosymmetric antiperovskite compounds (M_3N)Bi (M = Ca, Sr, and Ba) are three-dimensional topological insulators. This proposed family of materials is chemically inert and the lattice structure is well matched to important semiconductors, which provides a rich platform to easily integrate with electronic devices.

DOI: 10.1103/PhysRevLett.105.216406 PACS numbers: 73.20.At, 71.15.Dx, 71.18.+y, 73.61.Le

It is well known from condensed matter textbooks that materials can be classified into two classes, either conductors or insulators (semiconductors). The former has robust metallic states with a Fermi surface separating partially occupied and unoccupied electronic bands, whereas the latter possess a band gap by which occupied bands are separated from unoccupied bands. Very recently, a new class of materials called topological insulators (TI) have brought a surge of interest. TIs represent a new exotic quantum state of matter with a bulk gap, similar to ordinary insulators, but with a formation of robust metallic edge or surface states that are protected by time reversal symmetry [1–20].

Owing to extensive research thus far, several families of materials for TI have been proposed theoretically and confirmed experimentally. The first discovery is a two-dimensional TI in an HgTe based quantum well [5]. Subsequently, several three-dimensional binary materials have been found to be 3D TI [6–13]. For example, a family of Bi_2Te_3, Bi_2Se_3, and Sb_2Te_3 has a single Dirac-cone band at the surface [10–12]. Recently, a different family of ternary semiconducting Heusler compounds without inversion symmetry has been proposed with proper strain engineering [14–16]. Another type of ternary thallium-based III-V-VI_2 chalcogenides ($TlBiTe_2$ and $TlBiSe_2$) has been also proposed [17–20]. Indeed, these materials are distinguished from ordinary insulators by nontrivial topological invariants associated with the bulk electronic structure [2,6,7,13]. Moreover, their electronic structures are characterized by band inversion where electronic bands with opposite parity around the Fermi level are inverted by spin-orbit coupling (SOC). This band inversion guarantees TI to have an odd number of Dirac-cone-like dispersions crossing the Fermi level at the surface [2].

In this Letter, we predict theoretically a new family of materials for 3D TI realized in ternary antiperovskite compounds. Through first-principles calculations, we demonstrate that (M_3N)Bi (M = Ca, Sr, and Ba), taken as a prototype system, becomes a strong TI upon the application of a uniaxial strain within the ab plane. The occurrence of TI is first examined based on the band inversion mechanism, and then verified by direct calculations of surface electronic states. We also discuss other related materials of the same antiperovskite structure which are good candidates for 3D TI.

As shown in Fig. 1, the cubic antiperovskite (M_3N)Bi (M = Ca, Sr, and Ba) compounds [21] crystallize in the space group of $Pm\bar{3}m$ of No. 221 with nitrogen atom at the center of the cube surrounded by octahedrally coordinated six alkaline-earth M metal and by group 15 element Bi in the resulting voids of the cube. In this class of compounds, the outermost electronic shells for M, Bi, and N are all p orbitals ($3p^2$ for Ca, $4p^2$ for Sr, $5p^2$ for Ba, $6p^3$ for Bi, and $2p^2$ for N). From the electronic structure point of view, 16-valence electron compounds with the antiperovskite structure such as the present systems are expected to be a semiconductor because the electrons fully occupy the atomic orbitals satisfying the closed-shell condition.

To investigate the electronic band structures of these materials, we perform *ab initio* calculations within the density functional theory using the Perdew-Burke-Ernzerhof–type generalized gradient approximation and the projected augmented wave method implemented in the Vienna *ab initio* simulation package (VASP) [22,23], including relativistic SOC.

The calculated electronic band structures for cubic (Ca_3N)Bi with and without SOC are shown in Fig. 2. Without SOC, (Ca_3N)Bi has a direct energy gap of about 0.54 eV [Fig. 2(a)]. When SOC is included, a large shift occurs for both the conduction and valence bands, and the resulting band gap reduces significantly as small as about 30 meV [Fig. 2(b)], indicating that the SOC has a large impact on this type of materials. As seen in Fig. 2(a), without SOC the valence band maximum (VBM) at the

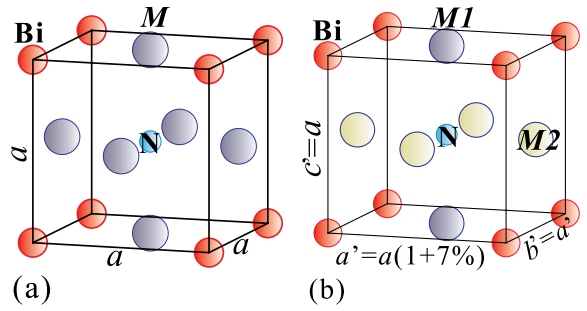

FIG. 1 (color online). Structure representations of cubic (a) and tetragonal (b) antiperovskite compounds $(M_3N)Bi$ (M = Ca, Sr, and Ba). In (b), the tetragonal distortion is along the [100] and [010] directions within ab plane. In cubic structure (space group $Pm\bar{3}m$ and point group O_h), M at $3c$ site $(1/2, 1/2, 0)$, N at $1b$ site $(1/2, 1/2, 1/2)$, and Bi at $1a$ site $(0, 0, 0)$. With the tetragonal distortion ($P4/mmm$, D_{4h}), M atoms become two inequivalent atoms, $M1$ at $1c$ site $(1/2, 1/2, 0)$ and $M2$ at $2e$ site $(1/2, 0, 1/2)$, as denoted in (b).

Γ point is a threefold degenerate Bi-$p_{(x,y,z)}$-like state, whereas the conduction band minimum (CBM) at the Γ point is a twofold degenerate Ca-d_{eg}-like state. Apparently, these threefold and twofold degeneracies are due to the cubic symmetry of the antiperovskite structure. By turning on SOC, the characters of the VBM and CBM change drastically and some of them are inverted. Namely, the VBM is now composed mainly by the Ca-d_{eg}-like states while the CBM is mainly by the Bi-$p_{(x,y,z)}$-like states.

The band inversion observed above is a strong indication for a potential TI. Based on the symmetry analysis, $(Ca_3N)Bi$ has four time reversal invariant momenta (TRIM), Γ, R, X, M, in the Brillouin zone. Following the parity criteria proposed by Fu and Kane [8], the topological invariants with the inversion symmetry can be classified by the product of the parity eigenvalues of the Bloch wave

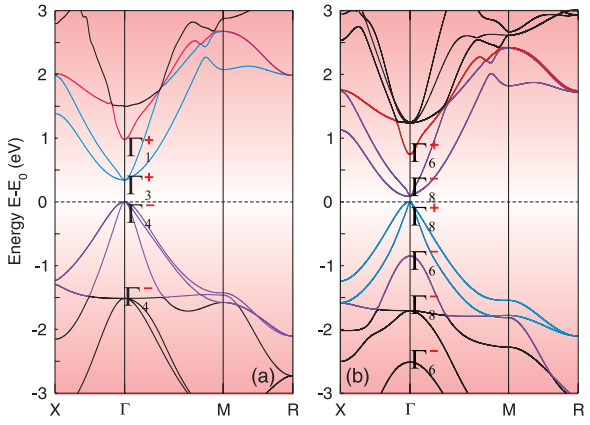

FIG. 2 (color online). Band structure for cubic $(Ca_3N)Bi$ without (a) and with (b) SOC. The lattice constants are taken from the optimized value (a = 4.921 Å). The dashed line indicates the top of valence band (E_0). The irreducible representations of O_h (a) and O_h' (b) at Γ are also indicated.

function for the occupied bands at TRIM. Our calculations found that the product of the parity eigenvalues of the totally six occupied valence bands at the Γ point is the same with or without SOC. We also found that the parity of the bands at the other three X, R, and M points do not change. Therefore, we conclude that cubic $(Ca_3N)Bi$ is a topologically trivial phase.

It is particular interesting that the band structure at around the Fermi level depends sensitively on the lattice distortion. To see this, we apply a uniaxial strain simultaneously along [100] and [010] directions to stretch or compress the ab plane while keeping the lattice constant along the c direction to the experimental one. This is similar to a real growth condition for thin films on proper substrates. Because of the tetragonal deformation, the Ca atoms in the cubic antiperovskite structure become two inequivalent atoms Ca1 and Ca2, as shown in Fig. 1(b). The resulting band structures and the level sequences around the Fermi level for the Γ point are shown in Fig. 3(b) where the stretching strain is applied to elongate a and b lattice constants by 7%. Comparing with the strain-free case [Fig. 3(a)], the threefold degeneracy of Bi-$p_{(x,y,z)}$-like states at VBM and the twofold degeneracy of Ca-d_{eg}-like states at CBM are lift due to the distorted crystal field effect [Fig. 3(b)]. The threefold degenerate valence bands are split into a twofold degenerate Bi-$p_{(x,y)}$-like state and a nondegenerate Bi-p_z-like state. Similarly, the twofold degenerate Ca-d_{eg}-like states are split into two nondegenerate Ca-$d^*_{x^2-y^2}$-like and Ca-$d^*_{z^2}$-like states, which are moved upward in energy higher than the Bi-s-like state. This is because the strain induced expansion in the ab plane reduces significantly the Coulomb repulsions for Bi-$p_{(x,y)}$ and Ca-$d^*_{x^2-y^2}$ states compared to Bi-p_z and Ca-$d^*_{z^2}$ states, respectively. It should be emphasized that as a result of this distortion, the unoccupied Bi-s-like band originally located at higher energy is now located at the bottom of the conduction band while the VBM consists of a Bi-p_z-like state. This is the most favorable condition for bands with opposite parity to be inverted once SOC is included.

To see whether the SOC causes the band inversion, we calculate the band structures for the lattice distorted case with the realistic SOC, and the results are shown in Fig. 3(c). It is clearly seen in Fig. 3(c) that the band inversion indeed occurs between Bi-p_z-like and Bi-s-like states at the Γ point, and now the Bi-s-like state becomes occupied. Furthermore, we observe the anticrossing feature for the highest valence band in the vicinity of the Γ point. Because of the inversion of the bands with opposite parity, the product of the parity eigenvalues of the occupied bands at the Γ point changes the sign. This is a sharp contrast to the cubic case [Fig. 2(b)] where the sign remains the same. Simultaneously, it is found that the parity eigenvalues for all occupied bands at the other three TRIM R, X, and M remain the same. Therefore, these results evidence that the distorted $(Ca_3N)Bi$ by the stretching strain in the ab plane

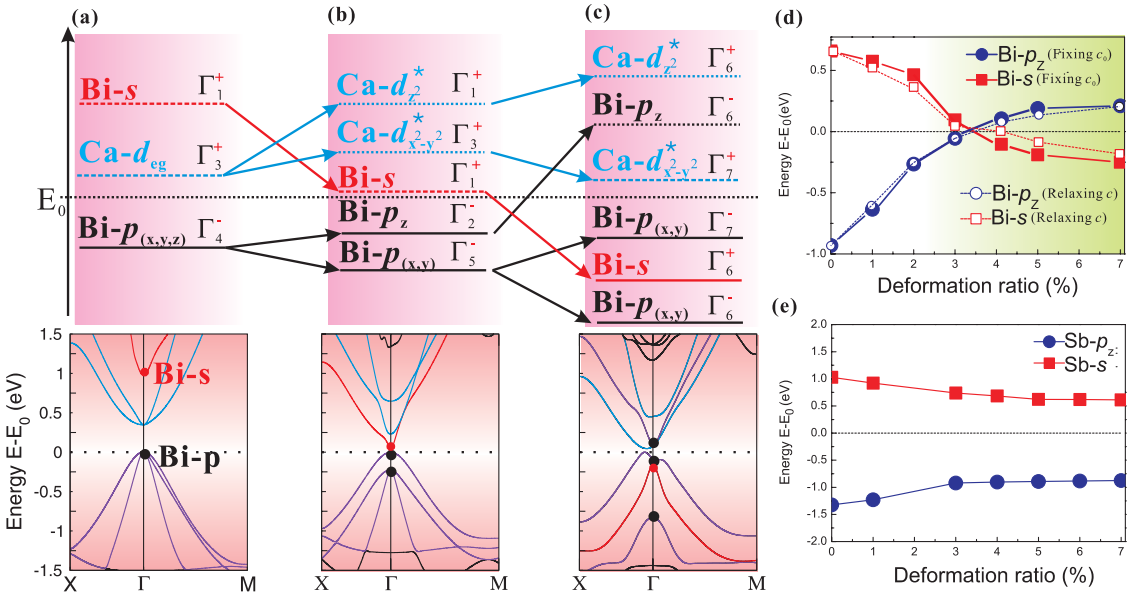

FIG. 3 (color online). (a) Band structures for cubic $(Ca_3N)Bi$ with the experimental lattice constants, and schematic energy level diagrams around the Fermi level at Γ. (b) The same as (a) but with an additional 7% tetragonal stretching distortion in the ab plane (see the text for details). (c) The same as (b) but with SOC. (d),(e) Energy levels at Γ for Bi (d) and Sb (e) p_z- and s-like states in $(Ca_3N)Bi$ (d) and $(Sr_3N)Sb$ (e) as a function of the deformation. In (d), hollow symbols refer to the structure with fully relaxed c axis at each deformation. In the upper panels of (a)–(c), the irreducible representations of O_h (a), D_{4h} (b), and D'_{4h} (c) for the bands at Γ are also indicated. Note that the antibonding Ca-d_{eg} orbital [(a)] in the cubic antiperovskite structure is split into Ca-$d^*_{x^2-y^2}$ and Ca-$d^*_{z^2}$ orbitals in the distorted tetragonal lattice [(b)].

is a 3D strong TI. In addition, we performed a series of calculations with SOC as a function of the deformation ratio, and found that the band inversion occurs when the stretching strain is larger than ~3% [Fig. 3(d)], for which $(Ca_3N)Bi$ is a 3D TI.

On the contrary, we found that the compression in the ab plane induces the same inverted band ordering but it turns the system to be semimetallic. In addition, we have also relaxed the lattice constant along the c direction while stretching the a and b directions so that zero stress is applied along the c direction. This situation is exactly the same as the real epitaxial condition of growth. Our results demonstrated that TI remains robust as long as the stretching strain is strong enough to elongate the lattice constants along the a and b directions by more than 3% [see Fig. 3(d)]. We further investigated the strain effect by a uniaxial strain along the [001] direction with a constant experimental volume. Stretching along the c axis makes $(Ca_3N)Bi$ semimetallic, whereas compressing along the c axis, which implies the expansion of both a and b axes, induces the system to be TI, as found above. For comparison, we also calculated the band structure for $(Ca_3N)Bi$ under hydrostatic strain. Obviously, the uniform compression causes the band gap to be larger while the cubic symmetry remains unchanged. Therefore, the resulting insulator is a topologically trivial band insulator. On the other hand, if the system is uniformly expanded (hydrostatic expansion), the semimetallic behavior is in turn observed.

The band inversion with opposite parities near the Γ point is clear evidence that the resulting state is a 3D TI. However, the most direct compelling evidence is the presence of the robust metallic surface states with odd number of bands crossing the Fermi level. Therefore, we study the (001) surface electronic band structures for cubic $(Ca_3N)Bi$ with no lattice distortions as well as for tetragonal $(Ca_3N)Bi$ with stretching strain in the ab plane of 7% lattice elongation. We take the charge-neutral slab with six unit cells (12 layers) with a 15-Å vacuum for surface calculations. Because of the sandwiched structure of CaBi and CaN layers, the (001) surfaces have two different terminations. We found that the CaBi exposed surface is energetically more favorable than the CaN surface. The obtained surface electronic band structures for $(Ca_3N)Bi$ without and with the stretching strain are shown in Figs. 4(a) and 4(b), respectively. It is clear from Fig. 4 that the strain-free cubic $(Ca_3N)Bi$ is a topological trivial phase because the number of bands crossing the Fermi level in momenta from $\bar{X}$ to $\bar{\Gamma}$ and from $\bar{M}$ to $\bar{\Gamma}$ is eight (even) [Fig. 4(a)]. For the stretched case, however, the number of bands crossing the Fermi level is odd (five in this case) [Fig. 4(b)], revealing that the system is a 3D TI.

We have calculated a series of other isostructural 16-valence electron nitrides composed of group 15 elements, $(M_3N)E$ (M = Mg, Ca, Sr, Ba; E = P, As, Sb, Bi) [24–27]. Under cubic symmetry with the experimental lattice constants and with no SOC, our band structure calculations

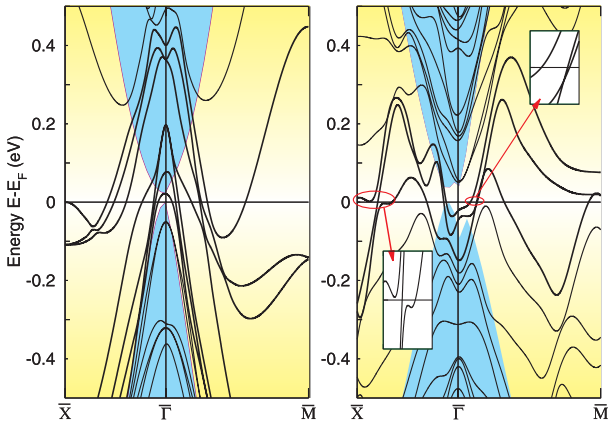

FIG. 4 (color online). Electronic band structures for (001) surface of $(Ca_3N)Bi$ with SOC. Left-hand panel: No strain applied. Right-hand panel: +7% stretching strain applied in *ab* plane while keeping the *c*-lattice constant fixed. The shaded regions indicate bulk energy bands.

found that these materials are all band insulators. With realistic SOC, it is found that $(Sr_3N)Bi$ and $(Ba_3N)Bi$ become 3D nontrivial TI either by a uniaxial strain along the [001] direction or by a strain simultaneously along the [100] and [010] directions in the *ab* plane. Without strain, these systems are trivial states. By contrast, our calculations show that it is difficult to realize 3D TI for the other nitrides $(M_3N)E$ (M = Ca, Sr, Ba; E = P, As, Sb) mainly because the SOC is not strong enough for P, As, and Sb to induce the band inversion. For instance, $(Sr_3N)Sb$ shows no band inversion between unoccupied Bi-*s*-like and occupied Bi-p_z-like states at the Γ point, at least, up to 7% stretching strain [Fig. 3(e)].

We have also studied another family of 16-valence electron antiperovskite oxides consisting of group 14 elements $(M_3O)E$ (M = Ca, Sr, Ba; E = Si, Ge, Sn, Pb) [28,29]. It is found that $(M_3O)Pb$ is a possible candidate for a 3D TI with proper strain engineering, whereas others $(M_3O)E$ (E = Si, Ge, Sn) are all trivial. It is interesting to note that, for all TI identified here in this Letter, the SOC causes the band inversion where the Bi-*s*-like state, which was unoccupied and located at a high-lying energy region without SOC, is pushed down to the top of the valence band once the SOC is included. This is an empirical rule that we acquired through this study in searching for TI in this family of materials.

Finally, we would like to emphasize that, from the crystallographic point of view, all known TI until now crystallize in two typical lattice structures, hexagonal and cubic phases. The former is centrosymmetric, such as Bi_2Se_3- and $TlBiTe_2$-type systems, whereas the latter is lack of inversion symmetry, such as zinc-blende HgTe type and its related one of ternary half-Heusler phases. The new family of materials proposed here in the antiperovskite structure is not only centrosymmetric but also cubic.

X.-Q. C acknowledges support from the "Hundred Talents Project" of CAS and the NSFC (Grant No. 51074151) as well as startup funding of the IMR. The calculations were partially performed on the SHENTENG 7000 CAS supercomputer in Beijing and on the National Supercomputing Center in Tianjin (TH-1 system).

*Corresponding author.
xingqiu.chen@imr.ac.cn

[1] J. E. Moore, Nature (London) **464**, 194 (2010).
[2] M. Z. Hasan and C. L. Kane, Rev. Mod. Phys. **82**, 3045 (2010).
[3] X.-L. Qi and S.-C. Zhang, Phys. Today **63**, No. 1, 33 (2010).
[4] X.-L. Qi, T. L. Hughes, and S.-C. Zhang, Phys. Rev. B **78**, 195424 (2008).
[5] B. A. Bernevig, T. L. Hughes, and S.-C. Zhang, Science **314**, 1757 (2006).
[6] J. E. Moore and L. Balents, Phys. Rev. B **75**, 121306 (2007).
[7] L. Fu, C. L. Kane, and E. J. Mele, Phys. Rev. Lett. **98**, 106803 (2007).
[8] L. Fu and C. L. Kane, Phys. Rev. B **76**, 045302 (2007).
[9] D. Hsieh *et al.*, Nature (London) **452**, 970 (2008).
[10] H. Zhang *et al.*, Nature Phys. **5**, 438 (2009).
[11] Y. Xia *et al.*, Nature Phys. **5**, 398 (2009).
[12] Y. L. Chen *et al.*, Science **325**, 178 (2009).
[13] R. Roy, Phys. Rev. B **79**, 195322 (2009).
[14] D. Xiao *et al.*, Phys. Rev. Lett. **105**, 096404 (2010).
[15] H. Lin *et al.*, Nature Mater. **9**, 546 (2010).
[16] S. Chadov *et al.*, Nature Mater. **9**, 541 (2010).
[17] H. Lin *et al.*, Phys. Rev. Lett. **105**, 036404 (2010).
[18] B. Yan *et al.*, Europhys. Lett. **90**, 37 002 (2010).
[19] Y. Chen *et al.*, arXiv:1006.3843.
[20] T. Sato *et al.*, Phys. Rev. Lett. **105**, 136802 (2010).
[21] F. Gäbler *et al.*, Z. Anorg. Allg. Chem. **630**, 2292 (2004). $(Ba_3N)Bi$ is known to crystallize in a hexagonal antiperovskite phase ($P6_3/mmc$). However, here we used an artificial cubic phase, similar to the experimental phase observed for both $(Ca_3N)Bi$ and $(Sr_3N)Bi$.
[22] G. Kresse and J. Hafner, Phys. Rev. B **48**, 13 115 (1993).
[23] G. Kresse and J. Furthmuller, Comput. Mater. Sci. **6**, 15 (1996).
[24] J. Jger *et al.*, Angew. Chem. **105**, 738 (1993).
[25] R. Niewa, W. Schnelle, and F. R. Wagner, Z. Anorg. Allg. Chem. **627**, 365 (2001).
[26] E. O. Chi, Solid State Commun. **121**, 309 (2002).
[27] P. R. Vansant *et al.*, Phys. Rev. B **57**, 7615 (1998).
[28] B. Huang and J. D. Corbett, Z. Anorg. Allg. Chem. **624**, 1787 (1998).
[29] C. Rhr, Z. Kristallogr. **210**, 781 (1995).